The impact of sea surface currents in wave power potential modeling

George Zodiatis, George Galanis, George Kallos, Andreas Nikolaidis, Christina Kalogeri, Aristotelis Liakatas & Stavros Stylianou

Ocean Dynamics
Theoretical, Computational and Observational Oceanography

ISSN 1616-7341

Ocean Dynamics
DOI 10.1007/s10236-015-0880-4

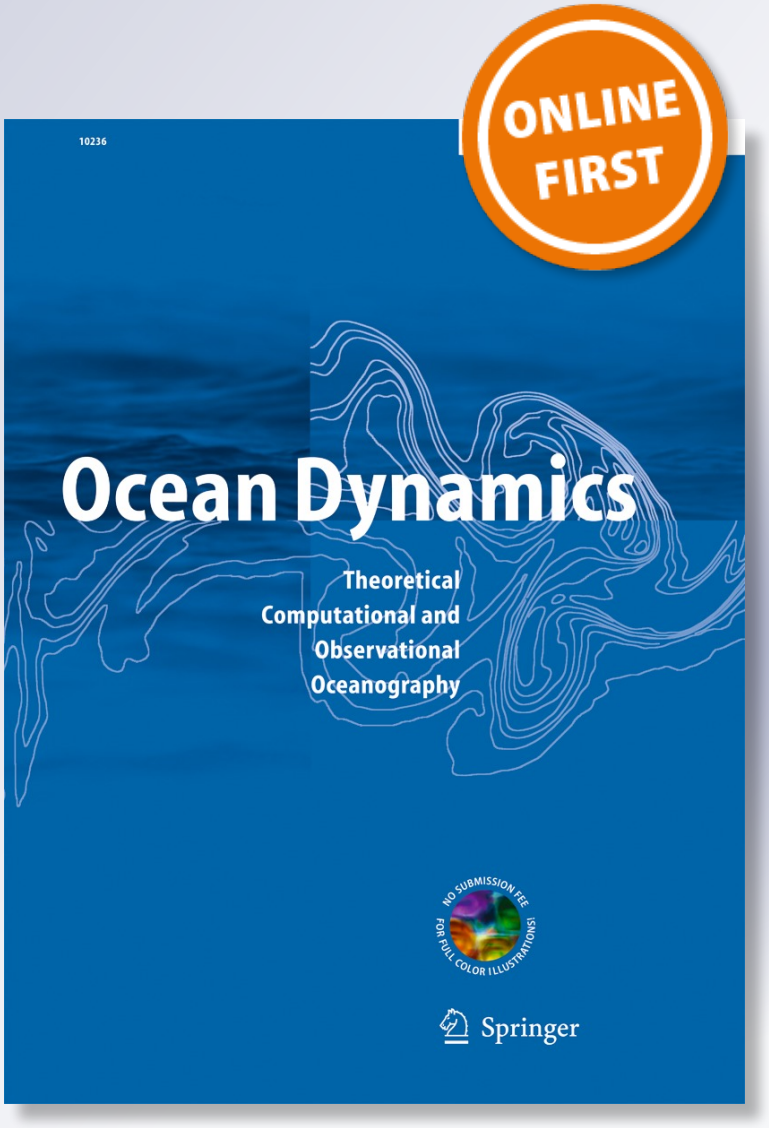

Springer

Ocean Dynamics
DOI 10.1007/s10236-015-0880-4

The impact of sea surface currents in wave power potential modeling

George Zodiatis[1] · George Galanis[2] · George Kallos[3] · Andreas Nikolaidis[1] · Christina Kalogeri[3] · Aristotelis Liakatas[2] · Stavros Stylianou[1]

Received: 6 February 2015 / Accepted: 3 September 2015

Abstract The impact of sea surface currents to the estimation and modeling of wave energy potential over an area of increased economic interest, the Eastern Mediterranean Sea, is investigated in this work. High-resolution atmospheric, wave, and circulation models, the latter downscaled from the regional Mediterranean Forecasting System (MFS) of the Copernicus marine service (former MyOcean regional MFS system), are utilized towards this goal. The modeled data are analyzed by means of a variety of statistical tools measuring the potential changes not only in the main wave characteristics, but also in the general distribution of the wave energy and the wave parameters that mainly affect it, when using sea surface currents as a forcing to the wave models. The obtained results prove that the impact of the sea surface currents is quite significant in wave energy-related modeling, as well as temporally and spatially dependent. These facts are revealing the necessity of the utilization of the sea surface currents characteristics in renewable energy studies in conjunction with their meteo-ocean forecasting counterparts.

Responsible Editor: Pierre De Mey

This article is part of the Topical Collection on *Coastal Ocean Forecasting Science supported by the GODAE OceanView Coastal Oceans and Shelf Seas Task Team (COSS-TT)*

✉ George Zodiatis
gzodiac@ucy.ac.cy

[1] Oceanography Centre, University of Cyprus, Nicosia 1678, Cyprus

[2] Mathematical Modeling Group, Section of Mathematics, Hellenic Naval Academy, 185 39 Hatzikiriakion, Piraeus, Greece

[3] Department of Physics, Atmospheric Modeling and Weather Forecasting Group, University of Athens, University Campus, Bldg. PHYS-V, 157 84 Athens, Greece

Keywords Wave modeling · Wave energy · Sea surface currents · Numerical meteo-ocean modeling

1 Introduction

Wave energy is an alternative renewable resource with critical advantages compared to other "clean" energy forms and very promising potential able to provide significant support to the worldwide efforts for reducing the dependency from oil-based power sources. The International Energy Agency in their 2010 annual report states that ocean energy has a potential to reach 3.6 GW of installed capacity by 2020 and close to 188 GW by 2050 (Brito-Melo and Huckerby 2010), while the global wave power resource has been estimated as around 2.1 TW (Gunn and Stock-Williams 2012). On the other hand, the nature of the wave energy makes it more feasible for integration into large grids due to its reduced variability, especially when compared with wind power, and its availability even in the absence of locally blowing winds over swell-dominated areas.

Today, many countries are working and investing on the growth of the wave energy technology supporting several R & D projects. Within this framework, a number of studies have been proposed for the last years: a European wave energy atlas has been presented by Pontes (1998) and Falnes (2007) focused on the wave spectrum parameters related to the distribution of wave energy; power installations in the Baltic and North Seas have been investigated by Henfridsson et al. (2007); the wave energy potential along the southeast US Atlantic coast has been studied by Defne et al. (2009); Iglesias et al. (2009) and Iglesias and Carballo (2009, 2010) analyzed the wave energy distribution in Spanish coastline; Arinaga and Cheung (2012) presented a 10-year hindcast modeling study; the energy potential in the Azores islands is the subject of Rusu and Soares (2012); The Black Sea area

Published online: 01 October 2015

was studied by a wave energy point of view in Akpınar and Kömürcü (2013); Vicinanza et al. (2013) focused on the area of Sardinia, Italy; Aoun et al. (2013) on Lebanon sea areas; Zodiatis et al. (2014) on the Levantine Sea area in the Eastern Mediterranean Sea, while corresponding studies for the European Atlantic coastline have been published by van Nieuwkoop et al. (2013) and Gonçalves et al. (2014) and for non-European areas by Hughes and Heap (2010); Hemer and Griffin (2010); Lenee-Bluhm et al. (2011);Stopa et al. (2011), Chiu et al. (2013), and Morim et al. (2014).

Despite the above-mentioned efforts in analyzing the wave power over different areas worldwide and although it is well known that sea surface currents have a non-trivial impact on the wave properties and local wave climatology (see for example Huang et al., 1972; Hedges 1987; Jonsson 1990; Soares and de Pablo 2006; Haus 2007; Mellor 2008; Brown and Davies 2009; JoãoTeles et al. 2013), only a few wave resource assessment studies have encountered wave-current interaction impact: Saruwatari et al. (2013) show that considerable changes in the wave climate may occur due to tidal impacts on waves leading even to 150–200 % in wave height and to a subsequent increase in wave power of over 100 kW/m. Belibassakis and Athanassoulis (2014) studied the transformation of the directional spectrum of an incident wave system over a region of strongly varying three-dimensional bottom topography and the corresponding impact to wave energy dissipation, Hashemi and Neill (2014) suggested that the impact of tides may exceed 10 % in some areas, while Barbariol et al. (2013) provide a wave energy assessment study in the Adriatic Sea based on a wave-ocean coupled system.

The main aim of the present work is to study the impact of sea surface currents to the wave energy potential over an area of increased scientific and economic interest: the Levantine basin in the Eastern Mediterranean Sea. The same region was the target area of Zodiatis et al. (2014) in which a general wave energy study has been provided without, however, taking into account any possible influence of the sea currents.

The presented approach is based on state-of-the art numerical modeling systems, able to simulate accurately and in high temporal and spatial resolution mode the evolution and the interaction of wind, waves, and sea currents. More precisely, the atmospheric model SKIRON (Kallos 1997; Papadopoulos et al. 2001; Spyrou et al. 2010), the latest version of the wave model WAM (WAMDIG 1988; Komen et al. 1994; Bidlot et al. 2007) and a new parallel version of the hydrodynamic model based on the Princeton Ocean Model (POM) (Blumberg and Mellor 1987; Mellor and Yamada 1982; Mellor 2003, Radhakrishnan et al. 2011, 2012) are utilized running on a very high spatial resolution (~0.01°) appropriate for revealing the potential interactions between waves and sea currents and the subsequent changes to the local wave power potential. Both the wave and hydrodynamic models are running under the Cyprus Coastal Ocean Forecasting System (CYCOFOS) providing daily operational forecasts at subregional and regional scales in the Eastern Mediterranean and the Mediterranean, respectively. The CYCOFOS hydrodynamic model is downscaled from the regional Mediterranean Forecasting System (MFS) system of the Copernicus marine service (former MyOcean regional MFS system).

A statistical analysis is also provided, based on a number of test cases that correspond to different wave conditions and are indicative of the local climatology, for analyzing by a qualitative point of view the impact of the sea surface currents on the wave power potential and on the main wave characteristics that affect it.

The obtained results show that there is indeed a non-trivial contribution of the sea surface currents to the estimation of the wave power potential, due to the fact that the significant wave height and the mean wave period, which are the two main parameters affecting the wave energy, can be significantly modified. The main findings, presented in Sections 3 and 4, reveal a clear difference of the wave and energy potential at the sea area between Cyprus and Egypt coastline. The wave power potential appears to reduce when sea surface currents are utilized in the wave modeling simulations to percentages reaching even 24 % of the reference values. At the same time, the distributions of significant wave height and mean wave period are also affected resulting to modified Hs/T joint probability distribution tables, a fact of importance for renewable energy resource assessment and applications.

The paper has been organized as follows: In Section 2, the numerical modeling systems, data sets, and area of interest are described. Section 3 contains the main information and results obtained while the conclusions reached are summarized in Section 4.

2 The study area and the models used

In this Section the general framework of the presented study is analyzed. The geographic region under consideration, the specific sites and time periods under study as well as the modeling tools employed are discussed.

2.1 The area and time period of interest

The area of interest in the present work is the Levantine basin in the eastern part of the Mediterranean Sea. Towards the analysis and study of the impact of sea surface currents to the wave energy potential, a number of test cases are presented based on the analysis of the wave characteristics and the corresponding wave energy potential itself. These cases cover a number of time periods of different wind/wave characteristics while the analysis is focusing on a series of locations with increased wave energy potential, according to the findings of Zodiatis et al. 2014, which provided a first in-depth estimation

of the wave energy potential in the same area of interest. The wind-wave characteristics are approached by means of state-of-the-art numerical atmospheric and wave models.

More precisely, several locations of interest, depicted in Fig. 1, are distributed along the coastline of Cyprus, Egypt, and Israel, while an offshore point also attracted our attention over the sea area of Eratosthenes SM, a region with increased wave power potential and a bathymetry that allows the development of wave energy platforms. The corresponding coordinates and bathymetry of the sites under study are presented in Table 1.

The analysis was performed for four different test cases that included typical weather patterns of the area under study in terms of wave direction and intensity. The time intervals of interest cover the following periods:

Test case 1: 17 March 2014 to 24 March 2014
Test case 2: 2 September 2013 to 5 September 2013
Test case 3: 15 October 2013 to 22 October 2013
Test case 4: 30 November 2013 to 14 December 2013

These cases have been chosen as indicative of the local climate covering different seasonal periods during spring (case 1), summer/autumn (cases 2/3), and winter (case 4). A more detailed description of the weather conditions during the selected cases follows:

Test case 1: This period is mainly characterized by calm to slight sea conditions with significant wave heights less than 1 m. The wave field is mainly from NW directions changing to western during the last days.
Test case 2: Slight to moderate (~1 m) is the prevailing wave conditions over the Eastern Mediterranean for this period. The main wave direction is from the NW.
Test case 3: During this period, the rather low values of significant wave height (less than 1 m) change to higher (~2 m). As for the directions, the wave field changes from NW to NE during the period of study.
Test case 4: The selected period starts with waves coming from the eastern sector with heights near to 1 m. During the next days, the wave field direction changed and was coming from the western sector. The sea conditions at that point became moderate to rough reaching even 3-m wave heights at specific locations.

It is important to underline that the main aim of the present study is the analysis of short-term changes to wave energy estimation when using the sea surface currents as a forcing, additionally to wind speed, in the wave model. For this reason, we avoided the analysis of extended data samples in which smoothing effects would be unavoidable (for example, short-term under- or overestimations would be summarized) and we focus on the study of short-term, indicative, test cases gave us the opportunity to reveal the, non trivial in several cases, impact that the use of surface currents have on the sea state simulation, especially on the corresponding wave power potential estimation.

2.2 The modeling tools

The wave numerical model used for wave analysis is the third-generation wave model WAM (WAMDIG 1988; Komen et al. 1994; Bidlot et al. 2007). In particular, the ECMWF version, CY36R4 (Janssen 2000, 2004) has been employed, supporting a number of important updates and potentials. The sea surface currents are introduced as a second forcing to the wave fields, besides the atmospheric forcing.

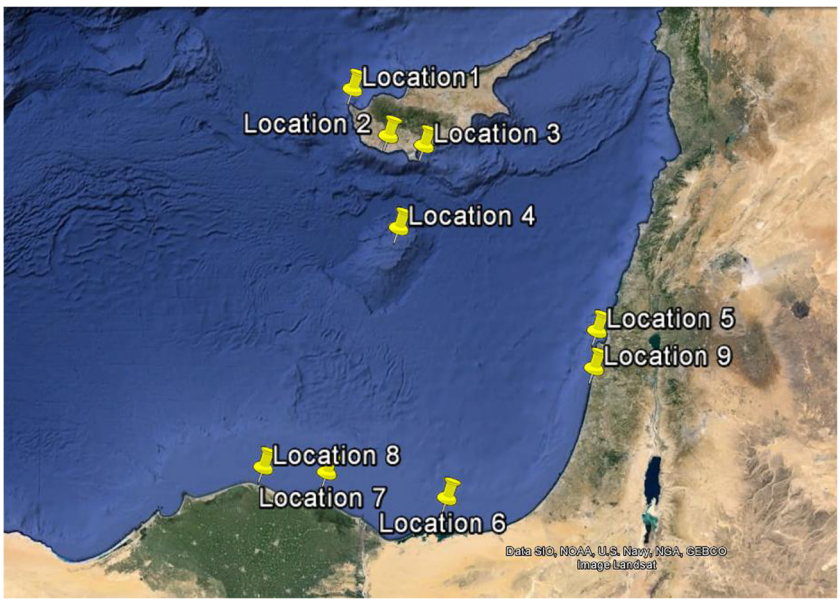

Fig. 1 The selected sites under study

Table 1 The sites selected for this study and the corresponding bathymetry

	Latitude	Longitude	Depth (m)
Location 1	35.100	32.250	74
Location 2	34.650	32.650	16
Location 3	34.550	33.050	433
Location 4	33.800	32.750	924
Location 5	32.800	34.900	48
Location 6	31.300	33.200	8
Location 7	31.550	31.900	5
Location 8	31.600	31.200	5
Location 9	32.450	34.850	30

The wave model's configuration includes a coarse domain covering the whole Mediterranean Sea (latitude 29 N–47 N, longitude 6 W–42 E, Fig. 2) at a horizontal resolution of 0.05×0.05° in order to capture and transfer as boundary conditions all the necessary swell information that affects the nested region of Levantine basin (latitude 31 N–37 N, longitude 30 E–36.5 E; red rectangle in Fig. 2), in which a horizontal high resolution of 1/60×1/60° has been adopted. To the authors' knowledge, this is the highest resolution used for operational wave forecasting in this region, providing an effective way to capture the local characteristics of waves, in contrast to previous wave energy studies of the area. For example, in Pontes (1998), the Mediterranean Sea was at a 0.5×0.5° resolution while Arinaga and Cheung (2012) worked with a 1.25×1° resolution.

The wave spectrum was discretized to 25 frequencies (range 0.0417–0.54764 Hz logarithmically spaced) and 24 directions (equally spaced) while the propagation time step has been set to 50 s for the nested Levantine basin high-resolution domain and at 150 s for the coarse Mediterranean one. The main characteristics of the wave model employed are summarized in Table 2.

WAM was driven by hourly wind input (10-m wind speed and direction) obtained from the SKIRON regional atmospheric system (Kallos 1997; Papadopoulos et al. 2001). The horizontal resolution used for the SKIRON model coincides with that of the wave model, while 45 vertical levels stretching from surface to 20 km altitude are employed. The SKIRON atmospheric system uses National Centers for Environmental Prediction (NCEP)/GFS 0.5×0.5° resolution fields for initial and boundary conditions. The necessary sea surface boundary conditions are interpolated from the 0.5×0.5° sea surface temperature (SST) field analysis retrieved from NCEP on a daily basis. Vegetation and topography data are applied at a resolution of 30 s and soil texture data with resolution of 120 s.

Since the quality of the atmospheric forcing always contributes to the credibility of wave simulations (see Ardhuin et al. 2007; Bolaños-Sanchez et al. 2007; Galanis et al. 2009; Papadopoulos and Katsafados 2009), it is important to

Fig. 2 The domains of the wave model: The coarser covers the Mediterranean and Black Seas while the second (denoted with the *red rectangle*) covers the high-resolution Levantine basin

Table 2 Wave model configuration

Wave model	WAM, ECMWF version CY36R4	
Area covered	Mediterranean Sea (29 N–47 N, 6 W–42 E)	Levantine Basin (31 N–37 N, 30 E–36.5 E)
Horizontal resolution	0.5×0.5°	1/60×1/60°
Frequencies	25 (range 0.0417–0.54764 Hz logarithmically spaced)	25 (range 0.0417–0.54764 Hz logarithmically spaced)
Directions	24 (equally spaced)	24 (equally spaced)
Timestep	150 s	50 s
Wind forcing	SKIRON atmospheric model	SKIRON atmospheric model
Wind forcing time step	1 h	1 h

underline that SKIRON is a well-established atmospheric forecasting system evaluated successfully in various research and operational projects: Such previous works have been presented for the area of Mediterranean Sea by Papadopoulos et al. (2001); Zodiatis et al. (2003, 2008); Papadopoulos and Katsafados (2009); and Galanis et al. (2011); for the Adriatic Sea by Dykes et al. (2009); the Aegean Sea by Korres et al. (2002); for issues relevant to renewable energy by Louka et al. (2008), Irigoyen et al. (2011), Correia et al. (2013), and Stathopoulos et al. (2013); for the Atlantic Ocean and oil spill modeling by Janeiro et al. (2012); for desert dust studies by Nickovic et al. (2001); Kallos et al. (2005); Balis et al. (2006); Spyrou et al. (2010); for air-quality applications by Astitha et al. (2005) and for photochemical processes by Varinou et al. (2000).

As already mentioned, the main aim of the present paper is to assess the effect of sea currents on the estimation of the wave's potential energy. The transmitted wave power per unit width is expressed by the formula:

$$P = 0.5 H_s^2 T_e (\mathrm{kW/m})$$

Sea currents can influence the wave generation mechanism and the wave propagation resulting in alterations in the wave energy spectrum and as a consequence in alterations in the integrated parameters of the spectrum, such as the significant wave height and the energy period (Huang et al. 1972, Jonsson 1990, Haus 2007, Soares and de Pablo 2006). Regarding the wave generation by wind, the presence of the current field may alter the relative velocity between air and water, which is either increased or decreased based on the sea current direction. This has a direct impact on the wave growth rate by affecting the effective fetch of the wind. For example, when winds and sea currents are coming from the same direction, waves do not grow as high as waves in still water (Peregrine 1976).

Wave propagation is also impacted by the ambient current. As waves move on a variable—in time and space—sea current field changes in amplitude, frequency, and direction occur. These changes can be attributed to the energy transfer between waves and sea currents, to the frequency shifting by the Doppler effect and to the sea current-induced refraction. In particular, when waves propagate against a sea current field, their wave lengths are shortened and their heights are increased. This growth is bounded by a frequency after which wave breaking occurs (Huang et al. 1972, Hedges 1987). On the other hand, when waves propagate along with the sea current field, the individual waves lengthen and their amplitudes are reduced. This results to a decrease, both in surface elevation and spectral density (Peregrine 1976, Rusu and Soares 2011, Saruwatari et al. 2013).

Moreover, the presence of sea currents may change the frequency of the waves due to the Doppler shift. More precisely, if the sea current speed U is positive (wave and sea current propagate in the same direction), then the frequency of waves is increased compared to what would be over still water. In the contrary, if U is negative (wave and sea currents propagate in opposite directions), then the frequency will be reduced.

In the present study the wave-sea current interactions are modeled by determining the evolution of the action density N

Table 3 Evaluation of the two versions of the wave model against in situ measurements

	WAM_NC – Buoy		WAM_C – Buoy	
	Mean bias (m)	RMSE (m)	Mean Bias (m)	RMSE (m)
Test case 1	0.05	0.16	0.06	0.16
Test case 2	0.28	0.33	0.31	0.36
Test case 3	0.10	0.29	0.14	0.32
Test case 4	0.19	0.42	0.19	0.41

Table 4 Evaluation of the two versions of the wave model against satellite records

	WAM_NC – Satellites		WAM_C – Satellites	
	Mean bias (m)	RMSE (m)	Mean bias (m)	RMSE (m)
Test case 1	0.13	0.34	0.13	0.34
Test case 2	−0.02	0.32	−0.02	0.32
Test case 3	0.04	0.46	0.04	0.46
Test case 4	0.44	0.63	0.44	0.64

$(x, t; s, \theta)$ in space x and time t by solving the action balance equation (Komen et al. 1994):

$$\frac{\partial N}{\partial t} + \nabla \boldsymbol{x}\left[(\boldsymbol{C_g} + \boldsymbol{U})N\right] + \frac{\partial C_\sigma N}{\partial \sigma} + \frac{\partial C_\theta N}{\partial \theta} = \frac{S_{\text{tot}}}{\sigma}$$

The action density (N) was selected instead of the energy density (E) because it is conserved during the propagation of the wave field in the presence of ambient current (Whitman 1974).

The left-hand side in the equation earlier is the kinematic part, while the right-hand part represents, through the source/sink terms, all the physical processes which generate, dissipate, or redistribute the wave energy. The first term from the left expresses the local rate of change of the wave action. The second term represents the 2-d geographical propagation of wave energy in x space. The propagation velocity is the result of the group (C_g) and the ambient currents velocity (U). The third term represents the shifting of the intrinsic frequency due to variations in depth and currents while the fourth term describes the depth and sea current-induced refraction effects. C_σ and C_θ are the propagation velocities in the spectral space and θ is the propagation direction.

In order to study the impact of the sea surface currents in the estimation of wave forecasts and the associated wave power potential, two versions of the earlier-described system were employed: One implementing the sea surface currents as a second forcing beyond the 10-m wind speed and direction (abbreviated for convenience as WAM_C) and one running without the impact of surface currents (WAM_NC).

For the former, data from the MFS regional Copernicus marine service (former MyOcean regional MFS) has been employed. In particular, the Mediterranean Forecasting System (Pinardi et al. 2003) provides operational forecasting data at a resolution of 1/16° for the coarse domain of the Mediterranean wave model. The MFS is consisting of a numerical model (Tonani et al. 2008) and the 3DVAR data assimilation scheme (Dobricic and Pinardi 2008) and provides operationally daily sea temperature, salinity, and sea current forecasts, with 10-day forecasting horizons at 6.5×6.5 km and 6-h temporal resolution.

The nested Levantine basin wave model domain is forced by sea surface currents provided by the new CYCOFOS parallel code hydrodynamical model nested to the regional MFS Copernicus marine service (former MyOcean regional MFS). More precisely, the new CYCOFOS flow model utilizes a

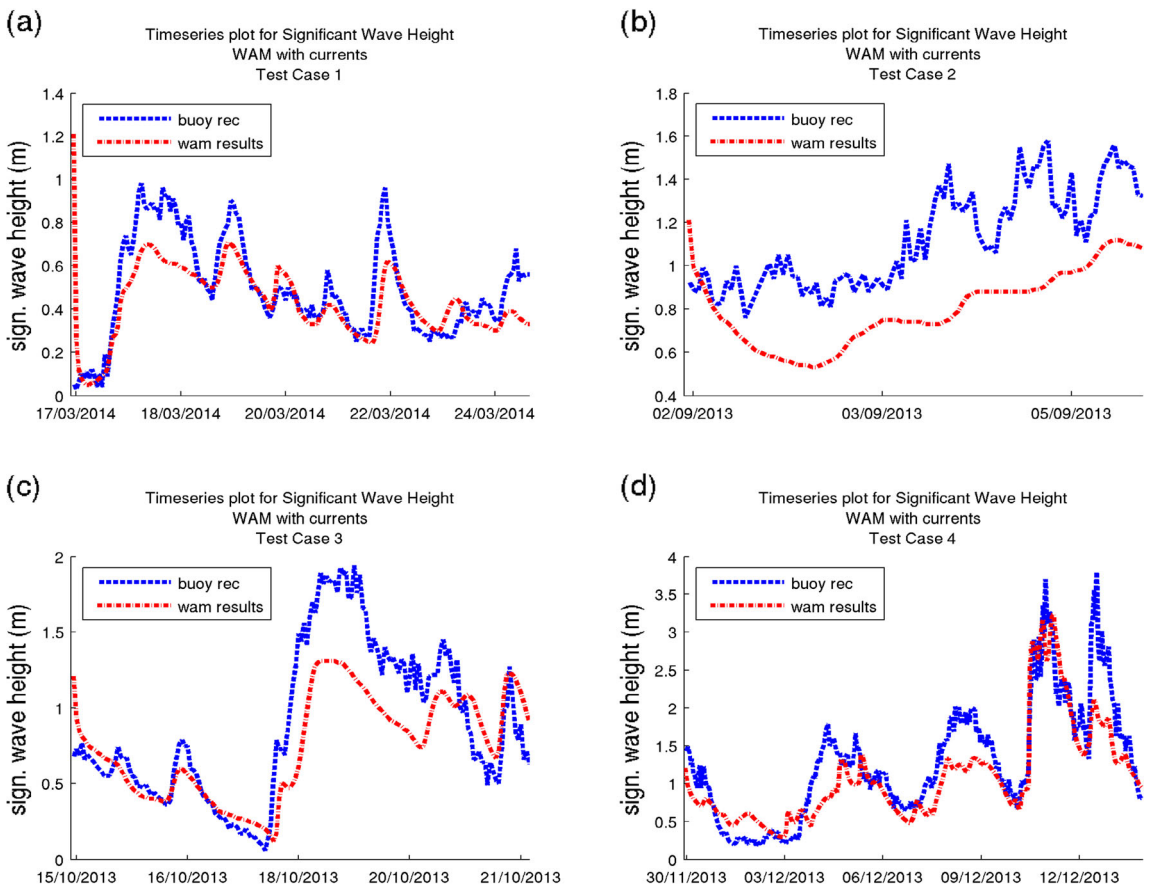

Fig. 3 Time Series of theWAM_C significant wave height values and the corresponding in situ wave measurements for the four test cases under study. **a** Test case 1. **b** Test case 2. **c** Test case 3. **d** Test case 4

distributed memory based on the message passing interface (MPI) paradigm (Radhakrishnan et al. 2011, 2012), aiming to provide operational oceanographic forecast and monitoring on local and subregional scales in the Eastern Mediterranean Basin. The model is using primitive equations in prognostic mode, sigma coordinate in vertical, Arakawa system in

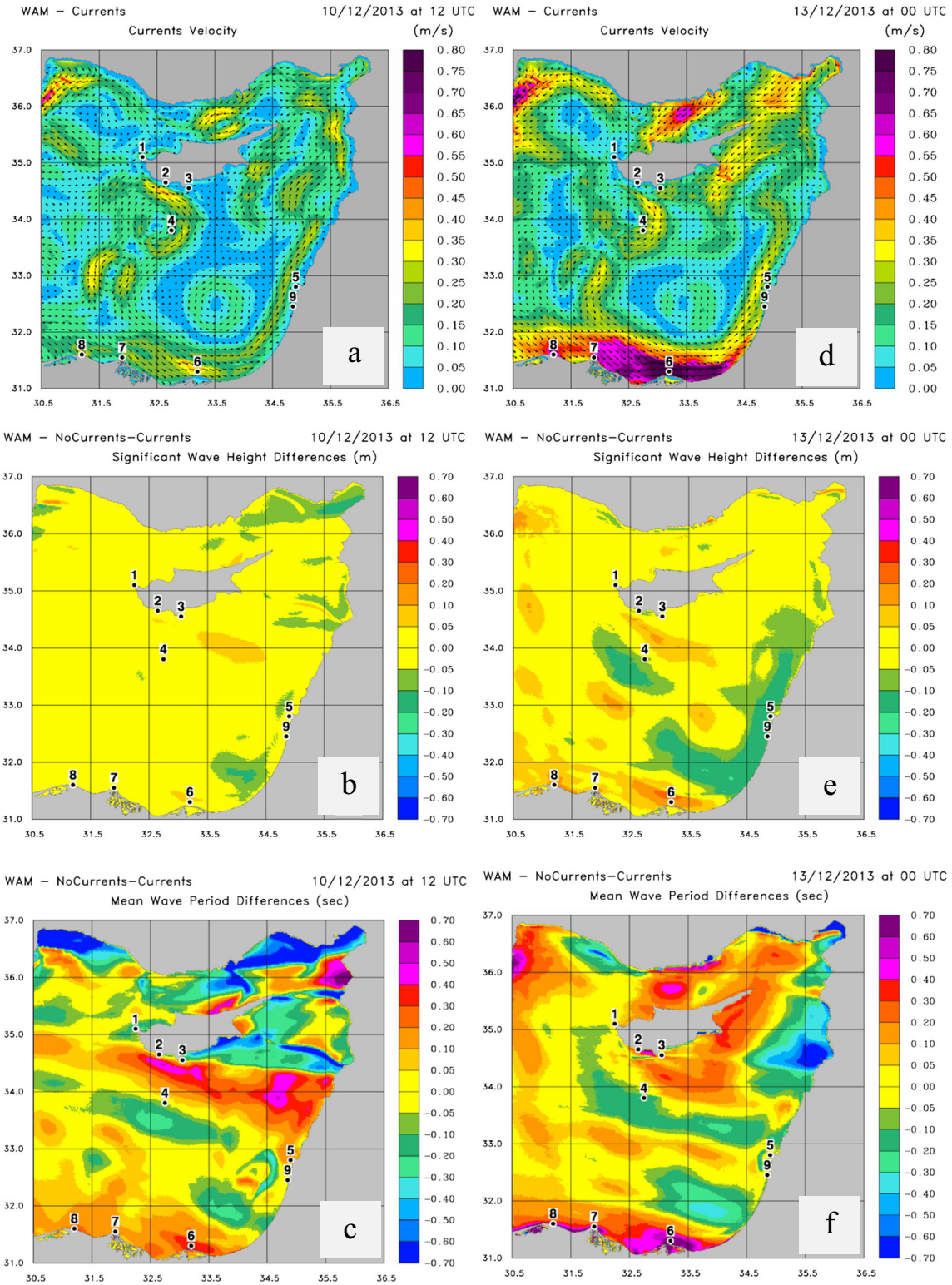

Fig. 4 Snapshots of two different time moments 10 December 2013 at 12 UTC (**a**–**c**) and 13 December 2013 at 00 UTC (**d**–**f**). The spatial distribution of the sea surface currents velocity (**a**, **d**) and of the differences recorded between the WAM_C and the corresponding WAM_NC outputs for significant wave height (**b**, **e**) and period values (**c**, **f**) are depicted

Table 5 Statistical analysis of WAM_NC and WAM_C outputs for Cyprus coastline (location 2) during test case 1

Descriptive statistics: no currents: [lat 34.65, lon 32.65] 170314–240314				
	Hs (m)	Energy per (s)	Peak per (s)	Wave power (kW/m)
Mean	0.37	4.29	4.91	0.36
St. dev.	0.14	0.86	1.04	0.36
Var. coeff	0.38	0.20	0.21	1.01
St. error	0.01	0.06	0.06	0.03
Skewness	1.35	0.24	0.29	3.42
Kurtosis	8.29	1.89	2.24	23.76
Descriptive statistics: currents: [lat 34.65, lon 32.65] 170314–240314				
	Hs (m)	Energy per (s)	Peak per (s)	Wave power (kW/m)
Mean	0.38	4.28	4.87	0.37
St. dev.	0.14	0.84	1.01	0.36
Var. coeff.	0.38	0.20	0.21	0.99
St. error	0.01	0.06	0.06	0.03
Skewness	1.32	0.13	0.13	3.36
Kurtosis	8.00	1.82	2.15	23.52

horizontal, time splitting (external barotropic mode restricted by CFL condition, internal-baroclinic). Horizontal mixing is governed by the Smagorinsky scheme. Vertical mixing is governed by second-order turbulent energy scheme of Mellor and Yamada.

2.3 Evaluation of the system

Before proceeding with the main analysis and results of the present study, it is important to discuss some basic evaluation facts for the wind-wave modeling system utilized in order to ensure the credibility of the modeled outcomes. The new version of the wave model WAM has been already successfully evaluated in a number of previous works (Bidlot et al. 2007; Bidlot 2012; Galanis et al. 2011; Emmanouil et al. 2012; Magnusson et al. 2013). However, additional indicative evaluation results for the test cases under study are presented here. To this end, two observation sources are employed: records from satellites over the area of interest and in situ measurements from a wave meter in the area of Hadera port, Israel.

More precisely, the remote sensing data are obtained from the altimeter sensors of three satellites: Cryosat-2, Jason-2, and SARAL (Satellite with ARgos and ALtiKa). Cryosat-2 and Jason-2 are in operation since April 2010 and June 2008, respectively, providing sea state data. They fly on low earth orbits at an altitude of 725 km for Cryosat-2 and 1336 km for Jason-2. Their period around the Earth is 99.16 and 112.57 min, respectively. They are able to monitor 95 % of oceans every 10 days approximately. On the other hand, Satellite SARAL is a cooperative altimetry technology mission of Indian Space Research Organization (ISRO) and the space agency of France (CNES). It is built by modules, one of which is the altimeter sensor Altika. This instrument is intended for oceanographic applications and as such it operates at 35.75 GHz. SARAL flies at a mean orbit altitude of 790 km with a period of 100.54 min at a sun synchronous orbit. Because of its higher operating frequency, it achieves an accuracy of 8 mm and spatial resolution of 2 km.

In general, the principle behind altimetry measurements is that the remote sensing (radar) instrument mounted on the satellite emits two electromagnetic pulses in two different frequencies and then measures the time needed for the pulses to

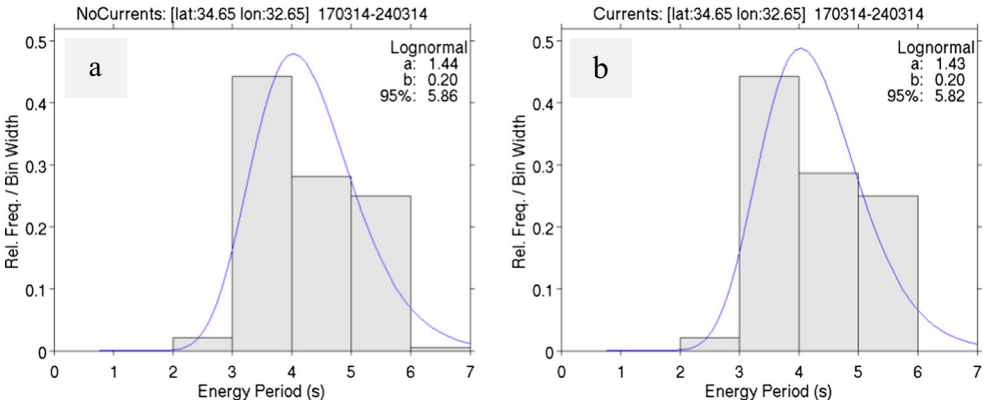

Fig. 5 Probability density function of the wave energy period of WAM_NC (**a**) and WAM_C (**b**) outputs for Cyprus coastline (location 2) during test case 1

Table 6 Statistical analysis of WAM_NC (a) and WAM_C (b) outputs for the Cyprus coastline (location 3) during test case 2

Descriptive statistics: no currents: [lat 34.55, lon 33.05] 020913–050913				
a	Hs (m)	Energy per (s)	Peak per (s)	Wave power (KW/m)
Mean	0.83	6.03	7.56	2.22
St. dev.	0.18	1.03	1.53	1.08
Var. coeff	0.22	0.17	0.20	0.49
St. error	0.02	0.10	0.10	0.11
Skewness	−0.31	−0.48	−0.42	0.48
Kurtosis	3.31	2.01	2.22	2.91
Descriptive statistics: currents: [lat 34.55, lon 33.05] 020913–050913				
b	Hs (m)	Energy per (s)	Peak er (s)	Wave power (kW/m)
Mean	0.87	6.06	7.34	2.44
St. dev.	0.18	1.02	1.34	1.13
Var. coeff.	0.21	0.17	0.18	0.46
St. error	0.02	0.10	0.10	0.12
Skewness	−0.49	−0.60	−0.96	0.23
Kurtosis	3.28	2.07	2.54	2.61

return. Thus, the range of the satellite from the surface of earth is estimated. In order to calculate the exact altimetry, the shape of the earth is referenced by an ellipsoid, while the satellite utilizes multiple positioning devices to accurately calculate its position. The difference between the distances measured by the radar and the one derived by the reference ellipsoid, results to the altimetry of a certain location. The resolution accuracy of these measurements is currently reduced down to a few centimeters (for more details, the reader is referred to Chelton et al. 2001).

The quality of measurements for significant wave height varies from 50 to over 80 % depending on limitations such as the presence of significant non-sea features in the altimeter footprint, like land or ice, days with heavy rain, or if the sea is glassy calm. Smaller objects such as ships do not significantly affect the measurement.

In addition, in situ wave measurements from the area of Hadera port in Israel are also utilized for evaluating our modeled wave data. This is a near-shore site (exact coordinates longitude 34.863057 latitude 32.47053) with sea depth of 27 m supported by the Israel Oceanographic and Limnological Research institute. In particular, hourly in situ significant wave height and mean wave period values are compared with the outcomes of the wave model.

It is also important to notice that the evaluation has been carried out over certain point locations in both cases. WAM provides as main output the 2-d wave spectrum $F(f,\vartheta,\varphi,\lambda)$ where f stands for frequencies, ϑ for directions, and (φ,λ) for over all latitudes and longitudes. The corresponding sea state characteristics—the significant wave height H_s and the energy wave period T_e _are obtained as integrated byproducts computed based on the moments of the wave spectrum:

$$H_s = 4\sqrt{m_0},\quad T_e = \frac{m_{-1}}{m_0}$$

where $m_n = \int_0^{2\pi}\int_0^{\infty} f^n E(f,\theta)\,df\,d\theta$, $n=-1, 0, 1, 2$.

The wave parameters are evaluated by means of the following statistical indexes:

$$\text{Mean bias: } \frac{1}{N}\sum_{i=1}^{N}(\text{obs}(i) - \text{mod}(i)),$$

Where obs stands for the observations and mod for modeled data and N for the sample size, revealing any possible

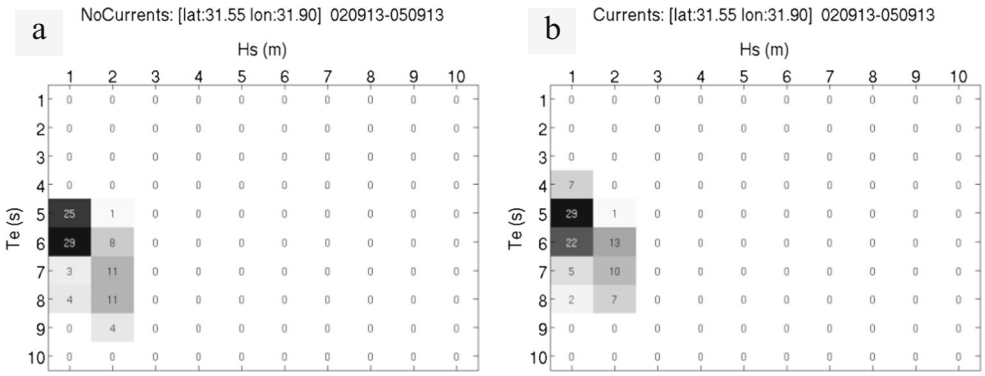

Fig. 6 Joint Hs/Te distribution of WAM_NC (**a**) and WAM_C (**b**) outputs for a point over the coastline of Egypt (location 7) during test case 2

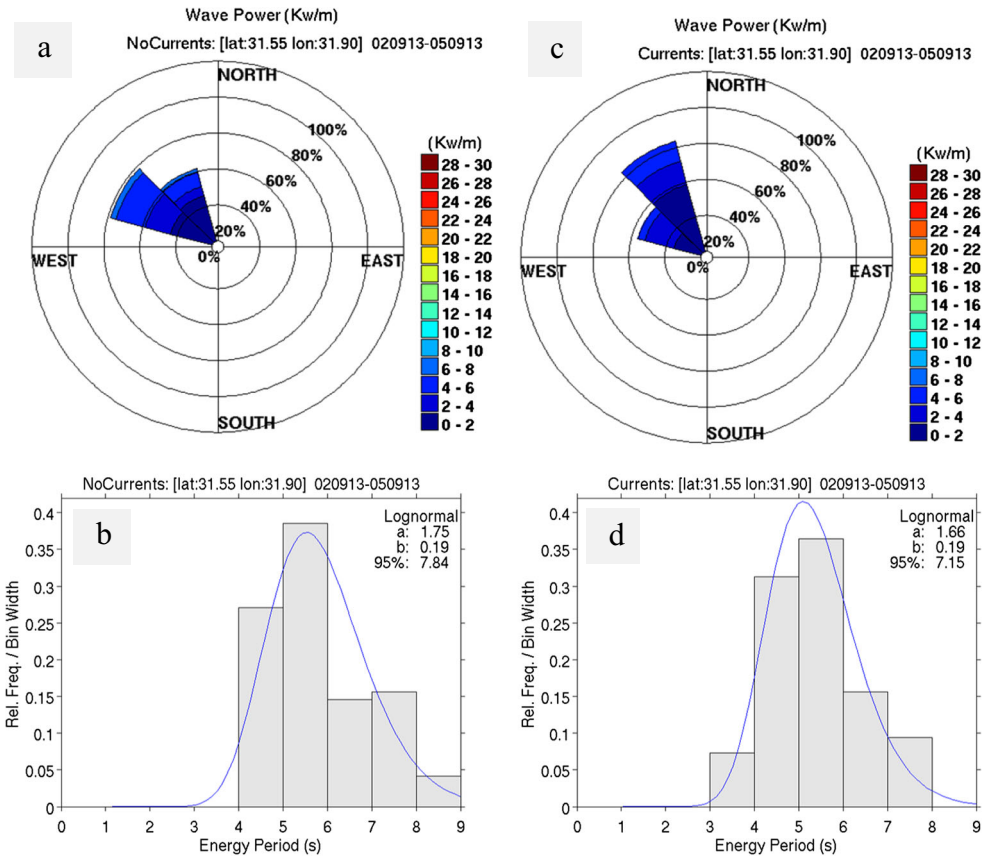

Fig. 7 Wave power roses of WAM_NC (**a**) and WAM_C (**c**) outputs for a point over the coastline of Egypt (location 7) during test case 2 and the corresponding probability distributions of mean wave period (**b**, **d**)

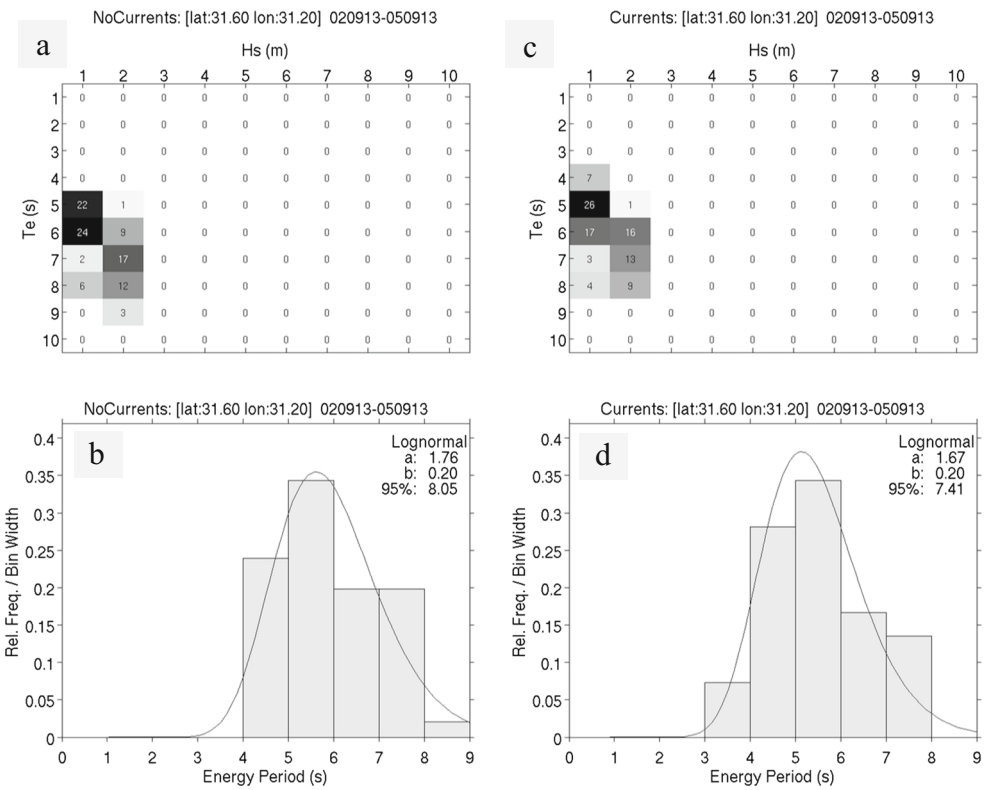

Fig. 8 Matrices of the joint Hs/Te distribution of WAM_NC (**a**) and WAM_C (**c**) outputs and the corresponding probability distribution function of mean wave period (**b**, **d**) for a second point along the coastline of Egypt (location 8) during test case 2

Table 7 Statistical analysis of WAM_NC (a) and WAM_C (b) outputs for a point over the coastline of Egypt (location 7) during test case 2

Descriptive statistics: no currents: [lat 31.55, lon 31.90] 020913–050913				
a	Hs (m)	Energy per (s)	Peak per (s)	Wave power (kW/m)
Mean	0.92	5.84	7.25	2.84
St. dev.	0.27	1.13	1.11	1.88
Var. coeff	0.29	0.19	0.15	0.66
St. error	0.03	0.12	0.12	0.19
Skewness	0.10	0.53	−0.82	0.53
Kurtosis	1.67	2.27	2.51	1.93
Descriptive statistics: currents: [lat 31.55, lon 31.90] 020913–050913				
b	Hs (m)	Energy per (s)	Peak per (s)	Wave power (kW/m)
Mean	0.86	5.37	6.89	2.23
St. dev.	0.23	1.01	1.00	1.39
Var. coeff.	0.27	0.19	0.14	0.62
St. error	0.02	0.10	0.10	0.14
Skewness	0.17	0.46	−0.79	0.49
Kurtosis	1.74	2.36	2.49	1.88

systematic discrepancies between modeled data and their corresponding measurements

Root mean square error (RMSE): $\sqrt{\frac{1}{N}\sum_{i=1}^{N}(\mathrm{obs}(i)-\mathrm{mod}(i))^2}$

providing information for the variability of the error.

In general, the statistics obtained (Tables 3 and 4) for the significant wave height evaluation over all the test cases performed and for both the observation sources are satisfactory: the mean bias values are low (from 0.02 to 0.44) proving that no systematic deviations were recorded, while the RMSE limited values—less than 0.63—reveal a rather low variability of the error too. Only in the second test case a more solid underestimation of the model can be mentioned.

The main conclusion reached for both wave systems running with (WAM_C) and without (WAM_NC) the sea surface currents impact is that they perform similarly well with almost no alterations in the bias and RMSE values.

This satisfactory performance of the wave model simulations is also depicted in Fig. 3 where the modeled significant wave height time series are compared with their corresponding in situ wave records (at the area of Hadera port) for the four test cases under study. An underestimation of the wave model outputs is noticed in some cases here but the limited magnitude of it (approximately 30 cm) should be underlined.

It should be noted, however, that the evaluation of a modeling system is always sensitive to the area applied and the configuration used. So, it is not surprising that there have been studies with even better evaluation statistical results for WAM (see for example Bidlot 2015), which however, refer to different regions and time periods. The important issue that one needs to keep from the present evaluation analysis is the satisfactory performance of the modeling systems adopted that supports the credibility of the main analysis and results on wave power estimation.

3 Results and analysis

In this section, the main findings of the present work are discussed towards the analysis of the impact of sea surface currents to the wave energy potential in the Eastern

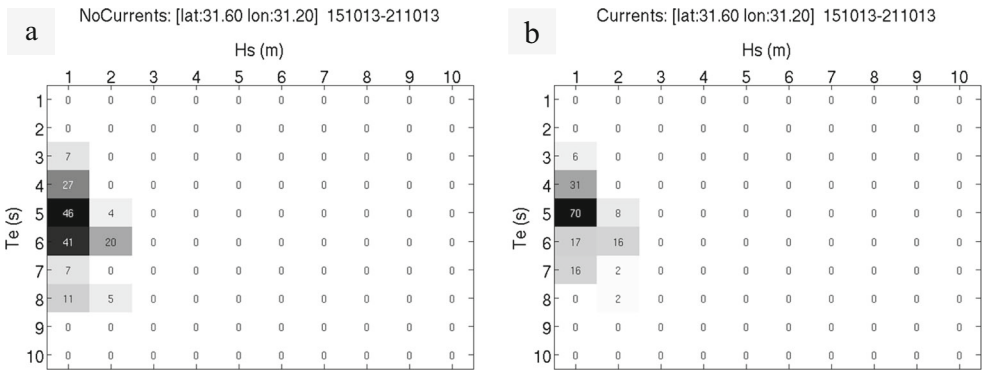

Fig. 9 Joint Hs/Te distribution of WAM_NC (**a**) and WAM_C (**b**) outputs for a point over the coastline of Egypt (location 8) during test case 3

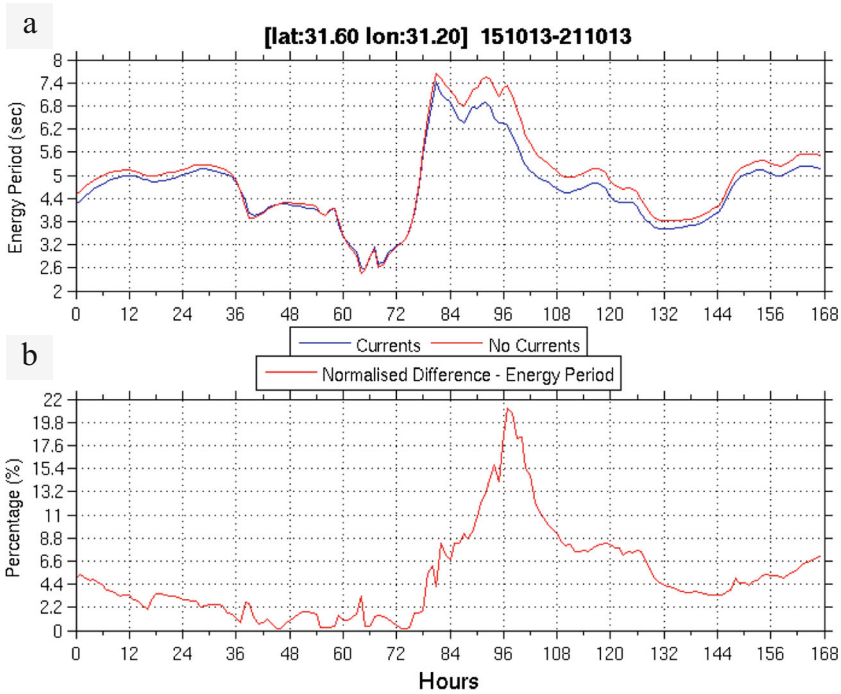

Fig. 10 Time series of mean wave energy period as modeled byWAM_NC (**a**, *red line*) and WAM_C (**a**, *blue line*) for a point along the coastline of Egypt (location 8) during test case 3 and the corresponding normalized differences (no currents-currents/ no currents) (**b**)

Mediterranean Levantine basin. Taking into account that the main associated wave parameters are the full 2-dimensional wave spectrum, the significant wave height, and the mean wave period, the presented outcomes focus mainly on the alterations recorded for these quantities in the presence of sea wave currents as a second forcing in the wave model.

3.1 Spatial analysis

It is worth initially noticing that when elevated surface wave values are recorded, both the significant wave height and the mean wave period, but especially the latter, differentiate at levels that may critically affect the wave energy potential. Indicative snapshots are depicted in Fig. 4, where the current velocity and the subsequent alterations on the wave height and period are presented as obtained by comparing the two different wave models used (with and without currents). Details on the spatial distribution of currents in the area can be found in Milena et al. 2012 and Pinardi et al. 2015).

3.2 Statistical analysis of the modeled outputs

Concerning the statistical analysis performed, a variety of indices are employed in order not only to reveal the main statistical components of the data under study but also to highlight critical characteristics related with potential impact of extreme values.

In particular, the following statistical measures were utilized:

Mean value: $\mu = \frac{1}{N} \cdot \sum_{i=1}^{N} x(i)$,

where x denotes the parameter in study and N the size of the sample;

Table 8 Statistical analysis of WAM_NC (a) and WAM_C (b) outputs for a point over the coastline of Egypt (location 8) during test case 3

Descriptive statistics: no currents: [lat: 31.60, lon 31.20] 151013–211013					Descriptive statistics: no currents: [lat 31.60, lon 31.20] 151013–211013				
a	Hs (m)	Energy per (s)	Peak per (s)	Wave power (kW/m)	b	Hs (m)	Energy per (s)	Peak per (s)	Wave power (kW/m)
Mean	0.66	4.92	6.09	1.42	Mean	0.64	4.68	5.87	1.28
St. dev.	0.34	1.13	1.72	1.43	St. dev.	0.32	0.98	1.55	1.28
Var. coeff	0.51	0.23	0.28	1.01	Var. coeff.	0.50	0.21	0.26	1.01
St. error	0.03	0.09	0.09	0.11	St. error	0.03	0.08	0.08	0.10
Skewness	0.45	0.47	0.57	1.28	Skewness	0.52	0.48	0.57	1.35
Kurtosis	2.61	3.23	2.82	3.50	Kurtosis	2.71	3.39	3.00	3.68

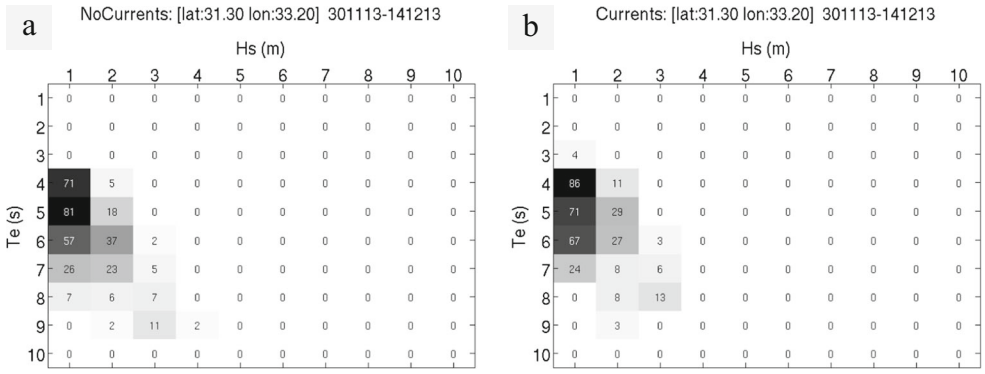

Fig. 11 Joint Hs/Te distribution of WAM_NC (**a**) and WAM_C (**b**) outputs for a point along the coastline of Egypt (location 6) during test case 4

Standard deviation: $\sigma = \sqrt{\frac{1}{N}\sum_{i=1}^{N}(x(i)-m)^2}$,

a typical variation index;

Skewness: $g_1 = \frac{\frac{1}{N}\cdot\sum_{i=1}^{N}(x(i)-\mu)^3}{\sigma^3}$,

a measure of the asymmetry of the probability distribution, and the kurtosis: $g_2 = \frac{\frac{1}{N}\cdot\sum_{i=1}^{N}(x(i)-\mu)^4}{\sigma^4} - 3$, measuring the "peakedness" of the probability distribution and the impact of possible extreme values. On the other hand, the modeled data were also approached by a distribution fitting, analyzing their full probability distribution.

The analysis is following the sequel defined in Section 2 by the test cases 1–4. During the spring test case 1 where a low (less than 1 m averaged) significant wave height was recorded, as a result of mild winds, and in the presence of low sea surface currents, minor alterations have been recorded in the distributions of significant wave height, mean wave period, and subsequently, in the wave energy potential. This is clearly depicted in Table 5 and Fig. 5 where the main statistical indices are presented. The only point that is worth mentioning is a slight translation of the right tail of the mean (energy) wave period to lower values.

Concerning the second test case which covers a summer period (September), the statistics in Table 6 indicate a slight increase of significant wave height values in the presence of sea wave currents, with subsequently elevated wave power values for the Cyprus coastline study region.

On the other hand, over the selected sites along the Egypt coastline, a direct impact of the sea current forcing is a reduction of the mean (energy) wave period values reaching a percentage of even 20 %. At the same time, the joint distribution of the two main wave parameters that affect the wave energy potential (significant wave height and mean wave period) is translated towards the reduced period values (Figs. 6, 7, 8 and Table 7). It is worth noticing that in all cases, the probability distribution function that optimally fits to the mean wave energy-modeled data is the 2-parameter lognormal.

Concerning test case 3 (Autumn–October period), trivial changes over the Cyprus and offshore sites were found after the use of sea currents as forcing to the wave model. However, for the triplet of Egypt sites, a non negligible reduction (up to 10 %) of the wave energy values is recorded as a consequence of the significant (up to 22 %) reduction of the mean wave period (Figs. 9, 10 and Table 8). At the same time, the right tail of the mean wave period distribution is eliminated.

Test case 4 seems to be the more interesting one being selected during winter months when the area under study is more active with several low pressure systems to pass over the

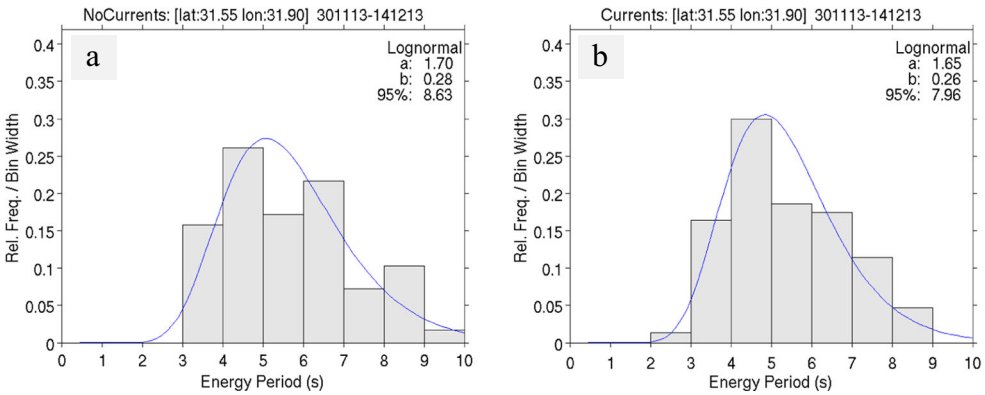

Fig. 12 Distributions of the mean (energy) wave period values of WAM_NC (**a**) and WAM_C (**b**) outputs for a point along the coastline of Egypt (location 7) during test case 4

Table 9 Statistical analysis of WAM_NC (a) and WAM_C (b) outputs for a point along the coastline of Egypt (location 6) during test case 4

Descriptive statistics: no currents: [lat 31.30, lon 33.20] 301113–141213				
a	Hs (m)	Energy per (s)	Peak per (s)	Wave power (kW/m)
Mean	0.98	5.22	6.31	4.03
St. dev.	0.58	1.27	1.82	6.47
Var. coeff	0.59	0.24	2.29	1.61
St. error	0.03	0.07	0.07	0.34
Skewness	1.43	0.72	0.16	2.94
Kurtosis	4.88	2.91	2.04	12.09
Descriptive statistics: currents: [lat 31.30, lon 33.20] 301113–141213				
b	Hs (m)	Energy per (s)	Peak per (s)	Wave power (kW/m)
Mean	0.93	4.90	6.01	3.11
St. dev.	0.51	1.18	1.86	4.67
Var. coeff.	0.55	0.24	0.31	1.50
St. error	0.03	0.06	0.06	0.25
Skewness	1.37	0.51	−0.01	2.94
Kurtosis	4.80	2.62	1.90	12.20

domain. The Egypt coastline points appear to have a remarkable reduction of the wave power potential values in the presence of sea surface currents in the wave model (WAM_C model version in which the MFS regional MyOcean data and the downscaled CYCOFOS hydrodynamic data have been utilized) as a result of corresponding mean wave period reduced values. This reduction reaches 24 % of the corresponding reference wave model values, as recorded in Figs. 11 and 12 and Tables 9 and 10, and is associated with analogous reduction of the deviation. The shape characteristics, however, of the corresponding distribution remain almost constant.

A further interesting note here is that gradients in the sea current speed seem to be related with ramps in the differences between the wave power estimated by the two wave model versions (Fig. 13), where the differences and the corresponding normalized values in wave power-modeled data by the two wave systems adopted are presented in conjunction with the significant wave height direction and the current speed. On the other hand, the sites close to the Cyprus coastline do not present significant variations when using sea surface currents as a forcing to the wave models (Fig. 14 and Table 11).

Additionally to the previous analysis and in order to give a longer term perspective of the wave characteristics that directly affect the wave power potential in the area under study, we present in Table 12 the basic statistics for the significant wave height and mean wave period for a full year (September 2013 – August 2014) period as simulated by the WAM model in which the currents impact has been taken into account.

Table 10 Statistical analysis of WAM_NC (a) and WAM_C (b) outputs for a point along the coastline of Egypt (location 7) during test case 2

Descriptive statistics: no currents: [lat 31.55, lon 31.90] 301113–141213				
a	Hs (m)	Energy per (s)	Peak per (s)	Wave power (kW/m)
Mean	1.05	5.69	6.96	6.62
St. dev.	0.81	1.58	1.86	13.73
Var. coeff	0.77	0.28	0.27	2.07
St. error	0.04	0.08	0.08	0.72
Skewness	1.96	0.47	−0.18	3.25
Kurtosis	6.63	2.29	2.69	13.25
Descriptive statistics: currents: [lat 31.55 lon 31.90] 301113–141213				
b	Hs (m)	Energy per (s)	Peak per (s)	Wave power (kW/m)
Mean	1.00	5.36	6.64	5.40
St. dev.	0.76	1.39	1.63	10.98
Var. coeff.	0.76	0.26	0.24	2.03
St. error	0.04	0.07	0.07	0.58
Skewness	1.96	0.37	−0.27	3.23
Kurtosis	6.61	2.19	2.95	13.15

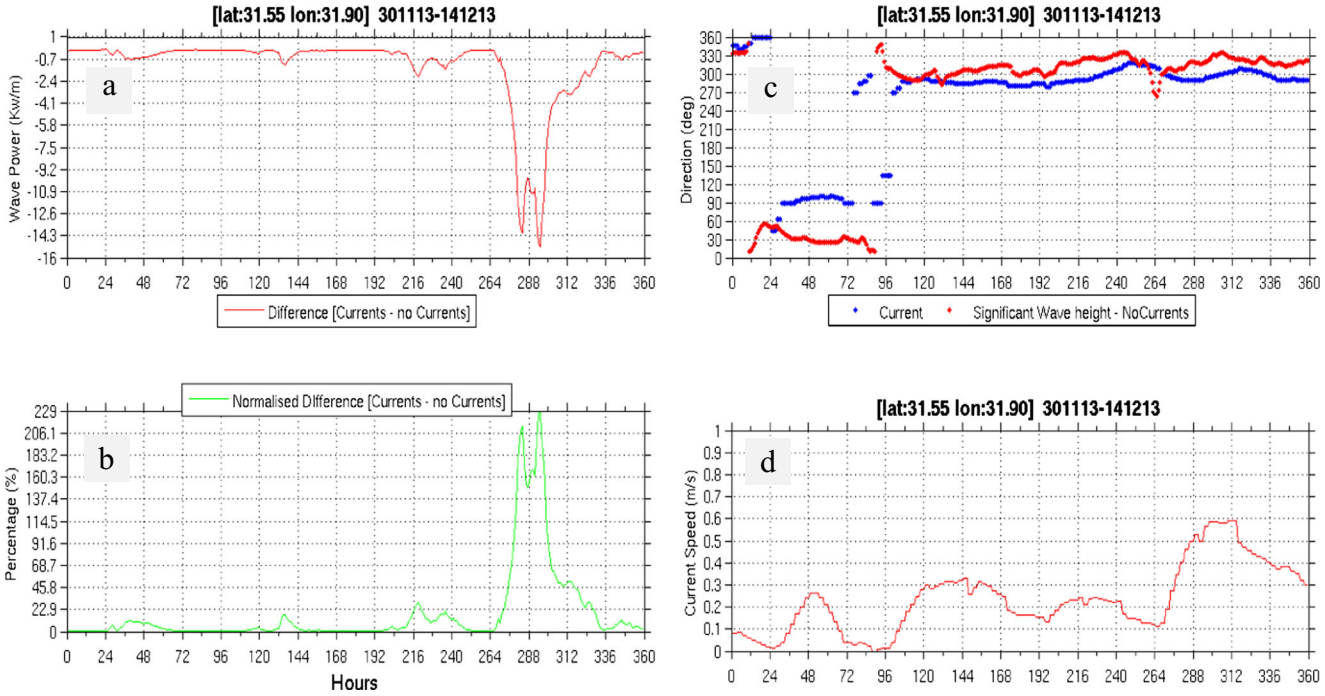

Fig. 13 Difference (**a**) and normalized difference (**b**) in wave power between WAM_NC and WAM_C outputs for a point (location 7) along the coastline of Egypt during test case 4. Currents and significant wave height direction (**c**) along with the time evolution of current speed (**d**) for the same location are also presented

This averaged information could be supportive for resource assessment purposes and the economic viability of offshore renewable energy projects.

3.3 Significance level of the sea surface currents impact to the wave model outputs

Closing this section, and since the main aim of the present study is to investigate the significance of the impact of sea surface currents to the sea state parameters that directly affect the wave power potential estimation, it is of interest to check the significance of the differences between the obtained modeled data by the two model versions employed (with and without the currents). To this end, the non-parametric Wilcoxon signed rank test (Wilcoxon 1945; Siegel 1956) is used to compare the wave power potential and the mean wave period data as modeled in the two different approaches. More precisely, the tests performed checked at a significance level of 95 % the null hypothesis of the non-significant differences between the modeled data. The results are presented in Table 13 and prove that the differences recorded is statistically significant in all points of all cases, except at the location with coordinates 34.55° N, 33.05° E and for the time period of test case 3. This fact further supports the importance of using sea surface currents in wave modeling systems.

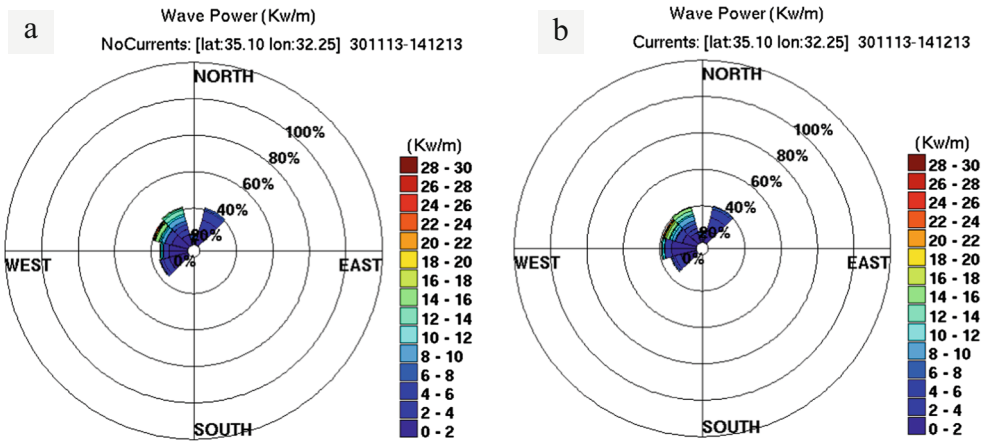

Fig. 14 Wave power roses of WAM_NC and WAM_C outputs for a point (location 1) close the coastline of Cyprus during test case 4

Table 11 Statistical analysis of WAM_NC (a) and WAM_C (b) outputs for a point (location 1) close the coastline of Cyprus during test Case 4

Descriptive statistics: no currents: [lat 31.30, lon 33.20] 301113–141213				
a	Hs (m)	Energy per (s)	Peak per (s)	Wave power (kW/m)
Mean	1.05	5.71	6.74	4.18
St. dev.	0.54	1.18	1.71	4.50
Var. coeff	0.52	0.21	0.25	1.08
St. error	0.03	0.06	0.06	0.24
Skewness	0.53	0.72	1.34	1.63
Kurtosis	2.41	4.62	5.98	5.53
Descriptive statistics: currents: [lat 31.30, lon 33.20] 301113–141213				
b	Hs (m)	Energy per (s)	Peak per (s)	Wave power (kW/m)
Mean	1.06	5.66	6.75	4.20
St. dev.	0.54	1.10	1.73	4.55
Var. coeff.	0.52	0.19	0.26	1.08
St. error	0.03	0.06	0.06	0.24
Skewness	0.55	0.34	1.18	1.60
Kurtosis	2.42	3.43	5.40	5.20

4 Conclusions

The main aim of the present work was to provide a study of the potential impact of sea surface currents to the wave energy potential over a high interest area with increased scientific and economical activities: the Levantine Basin in the Eastern Mediterranean Sea. In this way, the findings of previous studies on wave energy potential and assessment in the area (Vicinanza et al. 2013; Aoun et al. 2013; Zodiatis et al. 2014) are further supported taking into account the impact of wave-current interaction.

To this end, new high-resolution atmospheric, wave and ocean circulation numerical models were employed and their results, after evaluated for their accuracy against in situ and remote sensing wave observations, were analyzed by a wide number of statistical tools and indexes in order to reveal the added value of utilizing sea surface currents in conjunction with sea waves and wind for the estimation of wave forecasting and wave energy potential. The analysis provided was based on four indicative test cases which correspond to the main different seasonal periods of the area under study. The main findings can be summarized as follows:

- During periods of low wind speeds the impact of sea surface currents in the wave energy potential, but also on the two main wave parameters that affect it: the significant wave height and mean wave period, is limited. The only point that needs to be mentioned is a slight translation of the right tail of the mean wave period to lower values as well as a correspondingly slight increase of significant wave height with subsequent elevation of the wave power potential.
- For the same periods, interesting deviations from the above-mentioned general behavior is revealed for the Egypt coastline, where a much more significant impact of the induced sea currents is recorded leading to reduced wave period values at percentages of even 20 %.

Table 12 Statistical analysis of the significant wave height and mean wave period for one year period over the sites under study

Location	1	1	2	2	3	3	4	4	5	5	6	6	7	7	8	8	9	9
Parameter	Hs	Tm	Hs	Tm	Hs	Tm	Hs	Tm	Hs	Tm	Hs	Tm	Hs	Tm	Hs	Tm	Hs	Tm
Mean	0.75	4.99	0.64	4.89	0.75	4.71	0.87	4.85	0.68	5.03	0.51	4.22	0.46	4.17	0.46	4.23	0.70	5.01
StDev	0.55	1.25	0.49	1.41	0.54	1.35	0.63	1.28	0.58	1.36	0.29	1.01	0.35	1.31	0.34	1.37	0.60	1.39
Kurtosis	2.47	0.73	3.13	1.00	3.02	1.06	2.83	0.90	3.76	0.85	2.36	0.99	3.24	1.07	3.25	1.14	3.80	0.84
Skewness	12.07	3.30	18.26	3.63	17.75	3.68	14.44	3.48	22.18	3.44	10.80	4.08	19.27	3.99	18.22	4.16	23.01	3.54

Table 13 Significance tests for the differences between the outputs from WAM_NC and WAM_C models

	Test Case 1		Test Case 2		Test Case 3		Test Case 4	
	p-value	Statistically significant differences between WAM_NC - WAM	*p*-value	Statistically significant differences between WAM_NC - WAM	*p*-value	Statistically significant differences between WAM_NC - WAM	*p*-value	Statistically significant differences between WAM_NC - WAM
Location 1	0.00000	YES	0.00000	YES	0.00026	YES	0.00130	YES
Location 2	0.00000	YES	0.00000	YES	0.00027	YES	0.00000	YES
Location 3	0.00002	YES	0.00000	YES	0.12532	NO	0.00042	YES
Location 4	0.00029	YES	0.00000	YES	0.00014	YES	0.00037	YES
Location 5	0.00013	YES	0.00000	YES	0.00000	YES	0.00000	YES
Location 6	0.00000	YES	0.00000	YES	0.00000	YES	0.00000	YES
Location 7	0.00000	YES	0.00000	YES	0.00000	YES	0.00000	YES
Location 8	0.00000	YES	0.00000	YES	0.00000	YES	0.00000	YES
Location 9	0.00000	YES	0.00000	YES	0.00000	YES	0.00023	YES

- For the same area, the joint distribution of the significant wave height and mean wave period is crucially alternated in the presence of sea surface currents in the integration of the model. In particular, the modeled data with increased probability of occurrence seem to be shifted to reduced period values.
- In all cases, the mean wave energy is optimally fitted by the two-parameter lognormal distribution.
- The above-mentioned spatial differentiation between the Egypt coastline and the Cyprus near and offshore areas is even further underlined for the test periods of increased atmospheric and wave circulation during autumn and winter: Over Egypt waters, wave energy values are decreased in the presence of sea currents at percentages of even 24 %; a fact associated with similar reduction of the corresponding deviation values.
- The right tails of the wave period distributions almost disappear at the same time a fact revealing the reduction of higher/extreme period incidents.
- Gradients in the sea currents speed seem to be correlated with rapid changes in the wave power potential values.

As an overall conclusion, the non-trivial impact of the utilization of sea surface currents in wave power potential modeling simulations should be emphasized. This outcome reconfirms previous works (see for example Saruwatari et al. 2013; Belibassakis and Athanassoulis 2014; Hashemi and Neill 2014) performed over different areas and under different points of view on the necessity of taking into account wave-current interaction processes for wave energy assessment studies and underlines the added value of advanced/integrated modeling systems for resource assessment, designing, and operational relevant activities.

References

Ardhuin F, Bertotti L, Bidlot J, Cavaleri L, Filipetto V, Lefevre J, Wittmann P (2007) Comparison of wind and wave measurements and models in the Western Mediterranean Sea. Ocean Eng 34(3–4): 526–541

Akpınar A, Kömürcü M (2013) Assessment of wave energy resource of the Black Sea based on 15-year numerical hindcast data. Appl Energy 101:502–512

Arinaga R, Cheung KF (2012) Atlas of global wave energy from 10 years of reanalysis and hindcast data. Renew Energy 39:49–64

Astitha M, Kallos G, Mihalopoulos N (2005) Analysis of air quality observations with the aid of the source-receptor relationship approach. J Air Waste Manag Assoc 55:523–535

Aoun NS, Harajli HA, Queffeulou P (2013) Preliminary appraisal of wave power prospects in Lebanon. Renew Energy 53:165–173

Balis D et al (2006) Optical characteristics of desert dust over the East Mediterranean during summer: a case study. Ann Geophys 24:807–821

Barbariol F, Benetazzo A, Carniel S, Sclavo M (2013) Improving the assessment of wave energy resources by means of coupled wave-ocean numerical modeling. Renew Energy 60: 462–471

Belibassakis K, Athanassoulis G (2014) Gerostathis, directional wave spectrum transformation in the presence of strong depth and current inhomogeneities by means of coupled-mode model. Ocean Eng 87: 84–96

Bidlot J, Janssen P, Abdalla S, Hersbach H (2007) A revised formulation of ocean wave dissipation and its model impact. ECMWF Tech. Memo. 509. ECMWF, Reading, United Kingdom, 27pp. available online at: http://www.ecmwf.int/publications/

Bidlot JR (2012) Present status of wave forecasting at ECMWF. Proceedings from the ECMWF Workshop on Ocean Waves, 25–27 June 2012. ECMWF, Reading, United Kingdom

Bidlot JR (2015) Intercomparison of operational wave forecasting systems against buoys: data from ECMWF, MetOffice, FNMOC, MSC, NCEP, MeteoFrance, DWD, BoM, SHOM, JMA, KMA, Puerto del Estado, DMI, CNR-AM, METNO, SHN-SM January 2014 to December 2014 European Centre for Medium-range Weather Forecasts

Bolaños-Sanchez R, Sanchez-Arcilla A, Cateura J (2007) Evaluation of two atmospheric models for wind–wave modelling in the NW Mediterranean. J Mar Syst 65(1–4):336–353

Blumberg AF, Mellor GL (1987) A description of a three-dimensional coastal ocean circulation model. Three-Dimensional Coastal Ocean Models, edited by N. Heaps, 208 pp., American Geophysical Union

Brito-Melo A, Huckerby J (Eds.) (2010) Annual report 2010: implementing agreement on ocean energy systems. OES-IA

Brown JM, Davies AG (2009) Methods for medium-term prediction of the net sediment transport by waves and currents in complex coastal regions. Cont Shelf Res 29:1502–1514

Chelton DB, Ries JC, Haines BJ, Fu LL, Callahan PS (2001) Satellite altimetry, satellite altimetry and Earth sciences, L.L. Fu and A. Cazenave Ed., Academic Press

Chiu F, Huang W, Tiao W (2013) The spatial and temporal characteristics of the wave energy resources around Taiwan. Renew Energy 52: 218–221

Correia P, Lozano S, Chavez R, Loureiro Y, Cantero E, Benito P, Sanz Rodrigo J (2013) Wind Characterization at the Alaiz – Las Balsas experimental wind farm using high-resolution simulations with mesoscale models. Development of a "low cost" methodology that address promoters needs. EWEA-13 proceedings, Vienna, February 2013

Defne Z, Haas K, Fritz H (2009) Wave energy potential along the Atlantic coast of the southeastern USA. Renew Energy 34:2197–2205

Dobricic S, Pinardi N (2008) An oceanographic three-dimensional variational data assimilation scheme. Ocean Model 22:89–105

Dykes JD, Wang DW, Book JW (2009) An evaluation of a high-resolution operational wave forecasting system in the Adriatic Sea. J Mar Syst 78(suppl 1):S255–S271

Emmanouil G, Galanis G, Kallos G (2012) Combination of statistical Kalman filters and data assimilation for improving ocean waves analysis and forecasting. Ocean Model 59–60:11–23

Falnes J (2007) A review of wave-energy extraction. Mar Struct 20:185–201

Galanis G, Emmanouil G, Kallos G, Chu PC (2009) A new methodology for the extension of the impact in sea wave assimilation systems. Ocean Dyn 59(3):523–535

Galanis G, Chu PC, Kallos G (2011) Statistical post processes for the improvement of the results of numerical wave prediction models. A combination of Kolmogorov-Zurbenko and Kalman filters. J Oper Oceanogr 4(1):23–31

Gonçalves M, Martinho P, Soares CG (2014) Wave energy conditions in the western French coast. Renew Energy 62:155–163

Gunn K, Stock-Williams C (2012) Quantifying the global wave power resource. Renew Energy 44:296–304

Hashemi MR, Neill (2014) The role of tides in shelf-scale simulations of the wave energy Resource. Renew Energy 69:300–310

Haus BK (2007) Surface current effects on the fetch limited growth of wave energy. J Geophys Res 112(CO3003):15

Hemer M, Griffin D (2010) The wave energy resource along Australia's southern margin. J Renew Sustain Energy 2:15. doi:10.1063/1.3464753

Hedges TS (1987) Combinations of waves and currents: an introduction. Proc Inst Civ Eng 82(Part I):567–585

Huang NE, Chen DT, Tung CC, Smith JR (1972) Interactions between steady non-uniform currents and gravity waves with applications for current measurements. J Phys Ocenogr 2:420–431

Henfridsson U, Neimane V, Strand K, Kapper R, Bernhoff H, Danielsson O, Leijon M, Sundberg J, Thorburn K, Ericsson K, Bergman K (2007) Wave energy potential in the Baltic Sea and the Danish Part of the North Sea, with reflections on the Skagerrak. Renew Energy 32:2069–2084

Hughes M, Heap A (2010) National-scale wave energy resource assessment for Australia. Renew Energy 35(8):1783–1791

Iglesias G, Carballo R (2009) Wave energy resource along the Death Coat (Spain). Renew Energy 34:1963–1975

Iglesias G, Lopez M, Carballo R, Castro A, Fraguela JA, Frigaard P (2009) Wave energy potential in Galicia (NW Spain). Renew Energy 34:2323–2333

Iglesias G, Carballo R (2010) Wave energy resource in the Estaca de Bares area (Spain). Renew Energy 35:1574–1584

Irigoyen U, Cantero E, Correia P, Frías L, Loureiro Y, Lozano S, Pascal E, Sanz Rodrigo J (2011) Navarre virtual wind series: physical mesoscale downscaling wind WAsP. Methodology and validation. EWEC-11 European Wind Energy Conference, Brussels, Belgium, March 2011

Janeiro J, Martins F, Relvas P (2012) Towards the development of an operational tool for oil spills management in the algarve coast. J Coast Conserv 16(4):449–460

Janssen P (2000) ECMWF wave modeling and satellite altimeter wave data. In D. Halpern (Ed.), Satellites, Oceanogr Soc, pp. 35–36, Elsevier

Janssen P (2004) The interaction of ocean waves and wind. University Press, Cambridge, **300pp**

Jonsson IG (1990) Wave–current interactions. In: Le Mehaute B, Hanes DM (eds) The sea, chap 3, vol 9, part A. Wiley, New York

JoãoTeles M, Pires-Silva AA, Benoit M (2013) Numerical modelling of wave current interactions at a local scale. Ocean Model

Kallos G (1997) The regional weather forecasting system SKIRON. Proceedings, Symposium on Regional Weather Prediction on Parallel Computer Environments, 15–17 October 1997, Athens, Greece, 9 pp

Kallos G, Papadopoulos A, Katsafados P, Nickovic S (2005) Trans-Atlantic Saharan dust transport: Model simulation and results. J Geophys Res (111)

Komen G, Cavaleri L, Donelan M, Hasselmann K, Hasselmann S, Janssen P (1994) Dynamics and modelling of ocean waves. Cambridge University Press

Korres G, Lascaratos A, Hatziapostolou E, Katsafados P (2002) Towards an ocean forecasting system for the Aegean sea. Glob Atmos Ocean Syst 8(2–3):191–218

Lenee-Bluhm P, Paasch R, Özkan-Haller T (2011) Characterizing the wave energy resource of the US Pacific Northwest. Renew Energy 36(8):2106–2119

Louka P, Galanis G, Siebert N, Kariniotakis G, Katsafados P, Pytharoulis I, Kallos G (2008) Improvements in wind speed forecasts for wind power prediction purposes using Kalman filtering. J Wind Eng Ind Aerodyn 96:2348–2362

Magnusson L, Thorpe A, Bonavita M, Lang S, McNally T, Wedi N (2013) Evaluation of forecasts for hurricane Sandy, Technical Memorandum, No. 699, ECMWF

Mellor GL (2003) Users guide for a three-dimensional, primitive equation, numerical ocean model. POM

Mellor GL, Yamada T (1982) Development of a turbulent closure model for geophysical fluid problems. Rev Geophys 20:851–875

Mellor GL (2008) The depth-dependent current and wave interaction equations: a revision. J Phys Oceanogr 38:2587–2596

Milena M, Poulain P-M, Zodiatis G, Gertman I (2012) On the surface circulation of the Levantine sub-basin derived from Lagrangian drifters and satellite altimetry data. Deep-Sea Res I 65:46–58

Morim J, Cartwright N, Etemad-Shahidi A, Strauss D, Hemer M (2014) A review of wave energy estimates for nearshore shelf waters off Australia. Int J Mar Energy 7:57–70

Nickovic S, Kallos G, Papadopoulos A, Kakaliagou O (2001) A model for prediction of desert dust cycle in the atmosphere. J Geophys Res 106(D16):18113–18129

Papadopoulos A, Katsafados P, Kallos G (2001) Regional weather forecasting for marine application. Global Atmos Ocean Syst 8(2–3): 219–237

Papadopoulos A, Katsafados P (2009) Verification of operational weather forecasts from the POSEIDON system across the Eastern Mediterranean. Nat Hazards Earth Syst Sci 9:1299–1306

Peregrine D (1976) Interaction of water waves and currents. Adv Appl Mech 16:9–117

Pinardi N, Allen I, De Mey P, Korres G, Lascaratos A, Le Traon PY, Maillard C, Manzella G, Tziavos C (2003) The Mediterranean ocean forecasting system: first phase of implementation (1998–2001). Ann Geophys 21(1):3–20

Pinardi N, Zavatarelli M, Adani M, Coppini G, Fratianni C, Oddo P, Simoncelli S, Tonani M, Lyubartsev V, Dobricic S, Bonaduce A (2015) Mediterranean Sea large-scale low-frequency ocean variability and water mass formation rates from 1987 to 2007: a retrospective analysis. Prog Oceanogr 132:318–332

Pontes MT (1998) Assessing the European wave energy resource. Trans Am Meteorol Soc 120:226–231

Radhakrishnan H, Moulitsas I, Hayes D, Zodiatis G, Georgiou G (2012) On improving the operational performance of the Cyprus Coastal Ocean Forecasting System. Geophys Res Abstr 14, EGU2012-13144-1

Radhakrishnan H, Moulitsas I, Hayes D, Zodiatis G, Georgiou G (2011) Development of a parallel code for the Cyprus Coastal Ocean Forecasting System, the future of operational oceanography 2011, Hamburg, Germany

Rusu CL, Soares G (2011) Modelling the wave–current interactions in an offshore basin using the SWAN model. Ocean Eng 38:63–76

Rusu L, Soares G (2012) Wave energy assessments in the Azores islands. Renew Energy 45:183–196

Saruwatari A, Ingram D, Cradden L (2013) Wave–current interaction effects on marine energy converters. Ocean Eng 73:106–118

Soares CG, de Pablo H (2006) Experimental study of the transformation of wave spectra by a uniform current. Ocean Eng 33:293–310

Siegel S (1956) Non-parametric statistics for the behavioral sciences. McGraw, New York

Spyrou C, Mitsakou C, Kallos G, Louka P, Vlastou G (2010) An improved limited area model for describing the dust cycle in the atmosphere. J Geophys Res: Atmos 115 (D17)

Stathopoulos C, Kaperoni A, Galanis G, Kallos G (2013) Wind power prediction based on numerical and statistical models. J Wind Energy Ind Aerodyn 112:25–38

Stopa J, Cheung K, Chen YL (2011) Assessment of wave energy resources in Hawaii. Renew Energy 36(2):554–567

Tonani M, Pinardi N, Adani N, Bonazzi A, Coppini G, De Dominicis M, Dobricic S, Drudi M, Fabbroni N, Fratianni C, Grandi A, Lyubartsev S, Oddo P, Pettenuzzo D, Pistoia J and Pujol I (2008) The Mediterranean Ocean forecasting system, coastal to global operational oceanography: achievements and challenges. Proceedings of the Fifth International Conference on EuroGOOS 20–22 May 2008, Exeter, UK

Varinou M, Kallos G, Kotroni V, Lagouvardos K (2000) The influence of the lateral boundaries and background concentrations on limited area photochemical model simulations. Int J Environ Pollut 14: 354–363

Vicinanza D, Contestabile P, Ferrante V (2013) Wave energy potential in the north-west of Sardinia (Italy). Renew Energy 50:506–521

van Nieuwkoop JCC, Smith HCM, Smith GH, Johanning L (2013) Wave resource assessment along the Cornish coast (UK) from a 23-year hindcast dataset validated against buoy measurements. Renew Energy 58:1–14

WAMDIG, The WAM-Development and Implementation Group, Hasselmann S, Hasselmann K, Bauer E, Bertotti L, Cardone CV, Ewing JA, Greenwood JA, Guillaume A, Janssen P, Komen G, Lionello P, Reistad M, Zambresky L (1988) The WAM model—a third generation ocean wave prediction model. J Phys Oceanogr 18(12):1775–1810

Whitman GB (1974) Linear and non-linear waves. Wiley, New York, **636 p**

Wilcoxon F (1945) Individual comparisons by ranking methods. Biom Bull 1(6):80–83

Zodiatis G, Lardner R, Georgiou G, Demirov E, Manzella G, Pinardi N (2003) An operational European global ocean observing system for the eastern Mediterranean Levantine basin: the Cyprus coastal ocean forecasting and observing system. Mar Technol Soc J 37(3):115–123

Zodiatis G, Hayes D. R, Lardner R, Georgiou G. (2008) Sub-regional forecasting and observing system in the Eastern Mediterranean Levantine Basin: the Cyprus Coastal Ocean Forecasting and Observing System (CYCOFOS), CIESM Monographs no. 34 (F. Briand Editor), ISSN 1726–5886, 101–106

Zodiatis G, Galanis G, Nikolaidis A, Kalogeri C, Hayes D, Georgiou G, Chu PC, Kallos G (2014) Wave energy potential in the Eastern Mediterranean Levantine Basin. An integrated 10-year study renewable energy. Renew Energy 69:311–323